Monte Carlo PENRADIO software for dose calculation in medical imaging

Camille Adrien, Mercedes Lòpez Noriega, Guillaume Bonniaud, jean-marc bordy, Cindy Le Loirec, Bénédicte Poumarède

Monte Carlo PENRADIO software for dose calculation in medical imaging

Camille Adrien[1], Mercedes Lòpez Noriega[1], Guillaume Bonniaud[2], Jean-Marc Bordy[1], Cindy Le Loirec[1], and Bénédicte Poumarede[1]

[1]*CEA, LIST, F-91191 Gif-sur-Yvette, France*
[2]*Centre de Medecine Nucleaire du Morbihan, Centre Hospitalier Bretagne Atlantique et Centre d Oncologie Saint-Yves, F-56000 Vannes, France*

The increase on the collective radiation dose due to the large number of medical imaging exams has led the medical physics community to deeply consider the amount of dose delivered and its associated risks in these exams. For this purpose we have developed a Monte Carlo tool, PENRADIO, based on a modified version of PENELOPE code 2006 release, to obtain an accurate individualized radiation dose in conventional and interventional radiography and in computed tomography (CT). This tool has been validated showing excellent agreement between the measured and simulated organ doses in the case of a hip conventional radiography and a coronography. We expect the same accuracy in further results for other localizations and CT examinations.

KEYWORDS: Monte Carlo simulation, PENELOPE, Medical Imaging, Radiation Dose

I. Introduction

The significant rise of medical imaging exams in the past few years has led to an increase in the collective dose due to irradiation.[1–3] The medical physics community agreed that this increase must be accompanied by a strong understanding of the radiation dose and its associated risks.[4–7] A controversial article announced that around 1.5% of all cancers in the United States may be attributable to the radiation from computed tomography (CT) examinations.[5] Even if this is an overestimation, it points out the necessity of convenient tools to evaluate the associated dose of medical radiation.

Commonly, non-individualized indices are used to estimate the radiation dose (CT dose index (CTDI), dose-length product (DLP), dose-area product (DAP), entry dose, etc . . .). The effective dose was first introduced as a measurement of dose for radioprotection, reflecting the radiation detriment. However it is mainly used to directly compare various radiation types and exposures but doesn't reflect the actual absorbed dose.

Several programs, devoted to a range of applications, have been developed and provide the common dose index (CTDI, DLP, dose-surface product), organ and tissue absorbed and/or effective dose.

- For conventional radiography (CR): PCXMC estimates the organ dose, the effective dose and its associated risk in CR for 29 organs and various types of numerical phantoms.[8] XDOSE and CHILDDOSE are based on the same principle. The CALDose_X calculates the common dose index in radiology and estimates the organ doses.[9]

- For CT examinations: ImPACT, Eff-Dose[10] and Org-Dose[11] give CTDI and DLP for several CT. ImpactMC provides a dose delivered estimation after examination.[12] Several research teams use Monte Carlo (MC) simulations for CT examinations.[13–16] For instance, the Duke University Medical Center has developed a tool for estimating organ absorbed dose and effective dose based on the PENELOPE code and using adaptive anthropomorphic numerical phantoms.[16]

Most of already existing tools don't take the person biological specificities into account and thus, only provide common dose index and effective dose rather than an actual dose delivered. Therefore our goal is not only to gather in a single software all already proposed features but also to replace common dose index with actual organ absorbed dosis. For that purpose we decided to include in a new MC tool, PENRADIO, the possibility of introducing individual specificities in order to obtain personalized results. The present MC program, dedicated to medical x-ray imaging procedures, is based on a modified version of PENELOPE code 2006 release.[17] It allows the calculation of an accurate individualized radiation dose in voxelized numerical phantoms. We start by presenting the tools and validation methodology for CR and interventional radiography (IR) as well as preliminary results. Then, CT tool developments are shown.

II. Method

1. The PENRADIO Software

The PENRADIO software (Figure 1) is based on PENSSART, a software initially developed for safety in radiotherapy.[18] The program uses PENELOPE code 2006 release allowing for particle transport in voxelized geometries. The PENSSART

software is divided into three modules:

- The dose calculation module is the core of the program. It was designed to perform MC dose calculations within voxelized geometries. To add this new functionality to PENELOPE a specific main program was developed in C++. The physics initially developed in PENELOPE remain unchanged and a ray-tracing algorithm was added for efficient navigation in the voxelized geometry. Results are provided in the form of two output matrices storing the dose absorbed in the medium and the statistical uncertainty for each voxel. The dose absorbed in the medium can be expressed in eV/g/shower or in Gray. Normalization factors[19] are usually computed for simulation results conversion to absolute dose values. We have chosen another method to determine the absolute dose values. When a phase space file (PSF) is used as an input, we can use:

$$D_{abs,Gy} = 1.6 \cdot 10^{-19} \cdot 1000 \cdot N_{elec} \cdot D_{MC,eV/g/shw} \quad (1)$$

with N_{elec} the number of electrons corresponding to the mAs used for the image acquisition, thus:

$$N_{elec} = A \cdot s / 1.6 \cdot 10^{-19} \quad (2)$$

When an energy spectrum is used, the result is given as the absorbed dose per initial photons. In addition to the number of initial electrons provided by the examination acquisition protocol, the tube yield y_{TX}, ratio of photons leaving the tube to initial electrons impinging the anode, has to be determined. The absolute absorbed dose can hence be obtained as follows:

$$D_{abs,Gy} = 1.6 \cdot 10^{-19} \cdot 1000 \cdot N_{photons} \cdot D_{MC,eV/g/shw} \quad (3)$$

$$D_{abs,Gy} = 1.6 \cdot 10^{-19} \cdot 1000 \cdot y_{TX} \cdot N_{elec} \cdot D_{MC,eV/g/shw} \quad (4)$$

- The patient module allows the implementation of complex geometries. The user can convert quadratic geometries normally used in PENELOPE into voxelized geometries by using a routine provided in PENCT[20] (such geometries will be called pengeom2ct phantoms[1]). A conversion process to transform patient CT images into data usable by the MC dose computation module has also been implemented.[18]

- The radiation source module allows the simulation of different kinds of radiation source going from simple sources such as monoenergetic beams to more complex sources like PSF resulting from a complete MC modeling of the x-ray tube. To generate such PSF, the module uses the PENELOPE code with a new version of the main program PENMAIN in which the selective bremsstrahlung splitting was implemented for simulations efficiency increase.
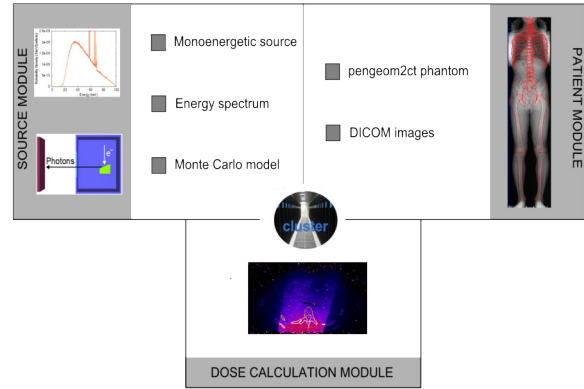
---

[1]F. Salvat: private communication

Figure 1: PENRADIO units and connections for dose calculation.

2. Dose calculation in CR and IR

In CR and IR information provided in the technical notes of the manufacturer is sufficient to perform a complete MC model of a X-ray tube.

2.1. Monte Carlo simulations

A CR tube (Philips DiDi TH2 CS4) and an IR tube (Philips MRC 200 0508 ROT-GS 1003) were simulated with PENELOPE according to the information provided in the technical notes. For the purpose of this study, several PSF corresponding to the maximal field size at the tube output were generated:

- two PSF for the 77 kVp and the 102 kVp of the CR tube;

- five PSF: four from 70 to 85 kVp by steps of 5 kVp and one for the 95 kVp for the IR tube.

Simulation with PENELOPE is controlled by different parameters: the absorption energies E_{abs} for electrons, photons and positrons, C_1 and C_2 determining the mean free path between hard elastic events and the maximum average fractional energy loss in a single step, W_{CC} and W_{CR} which are cutoff energies for hard inelastic interactions and hard bremsstrahlung emissions respectively. The simulation parameters are defined as a function of E_{max}, the maximum energy of the electron such as $E_{abs,electron} = E_{abs,positron} = E_{max}/100$, $E_{abs,photon} = E_{max}/1000$, $W_{CC} = E_{max}/100$, $W_{CR} = E_{max}/1000$, $C_1 = C_2 = 0.2$ for anode material and 0.1 for others.

2.2. Validation of the MC models

The main parameters of the MC model have been adjusted and validated using half value layers (HVL). The UNFORS detector has been used to measure the HVL of each simulated beam. The measurements have been compared with MC simulations performed with several aluminium filtrations. For each filtration the air Kinetic Energy Released per unit MAss (KERMA) has been calculated. Plotting air KERMA variations as a function of the aluminium filtration allows HVL determination.

2.3. Simulation of organ doses

Physical anthropomorphic phantoms (CIRS ATOM dosimetry phantoms) and their DICOM images have been used to compare measured and simulated radiation doses in the case of a hip CR (Table 1) and in the case of a cardiac IR (Table 2). Measurements were performed with Optically Stimulated Luminescence (OSL) dosimeters[21] while the PENRADIO software was used to determine the dose in some organs of interest.[22,23] Information about the calibration and the correction of the OSL readings is reported in the Appendix.

HighVoltage (kVp)	Charge (mAs)
77	25.2
102	6.91

Table 1: CR acquisition tube parameters.

HighVoltage (kVp)	Charge (mAs)	Acquisition Mode
73	154	Graphy
70	100	Graphy
73	128	Graphy
73	64	Graphy
74	89	Graphy
93	13	Scopy
72	101	Graphy
77	165	Graphy
74	119	Graphy

Table 2: IR acquisition tube parameters.

3. Tool adaptation for CT exams

The full MC modeling of the GE Lightspeed VCT 64 CT tube is impossible with the information provided in the technical notes of the manufacturer, especially because of the particular shape of the bowtie filters. To overcome this problem, we have implemented in C++ the method proposed by Turner et al.[24] Their study presents a method for generating x-ray source models based on experimental data. The so-called "Turner method" enables us to get equivalent spectra and bowtie filters.

3.1. Experimental determination of the X-ray tube spectrum

The equivalent inherent filtration of the tube has been determined using a program based on Turner[24] work. Three inputs are mandatory to run the developed program:

a) the first and second half value layers (HVL_1 and HVL_2);

b) an initial tungsten anode x-ray energy spectrum;

c) an arbitrarily chosen material used for filtration.

The following steps, reported in the flowchart in Figure 2, are used to get an equivalent spectrum:

1. The input energy spectrum is filtered assuming exponential attenuation by an initial thin sheet of aluminium (IF) providing a candidate spectrum and its associated KERMA (K_0).

2. Then the candidate spectrum is repetitively filtered by increasing the aluminium sheet thickness (AF) and its associated KERMA (K_1) is calculated until $K_0 = 2.K_1$. The simulated HVL_1 is set to the global additional sheet thickness used to verify this condition.

3. The second step is repeated to evaluate the simulated HVL_2 which fulfils the condition $K_0 = 4.K_2$.

4. Then comparison between experimental and computed data has to be made: either only HVL_1 values are compared (Method A) or the sum of both HVL_1 and HVL_2 values (Method B). If experimental and simulated data are similar, the equivalent spectrum is found. Otherwise, a new thicker initial sheet of aluminium is tested (step 1).

To run the Turner method we chose to use two different spectra to initialize the process, one softly filtered obtained with the Spekcalc tool,[25] the other unfiltered using MC simulation in order to compare the influence of the primary spectrum in the simulation process. MC simulation using PENELOPE based on the technical notes provides both the MC spectrum and the PSF of the CT head. PSF matches a 4 cm x 50 cm field size at a distance of 54.1 cm from the source for the 120 kVp voltage. The simulation parameters are defined as $E_{abs,electron} = E_{abs,positron} = 1000$ eV, $E_{abs,photon} = 100$ eV, $W_{CC} = W_{CR} = 100$ eV and $C_1 = C_2 = 0.2$.
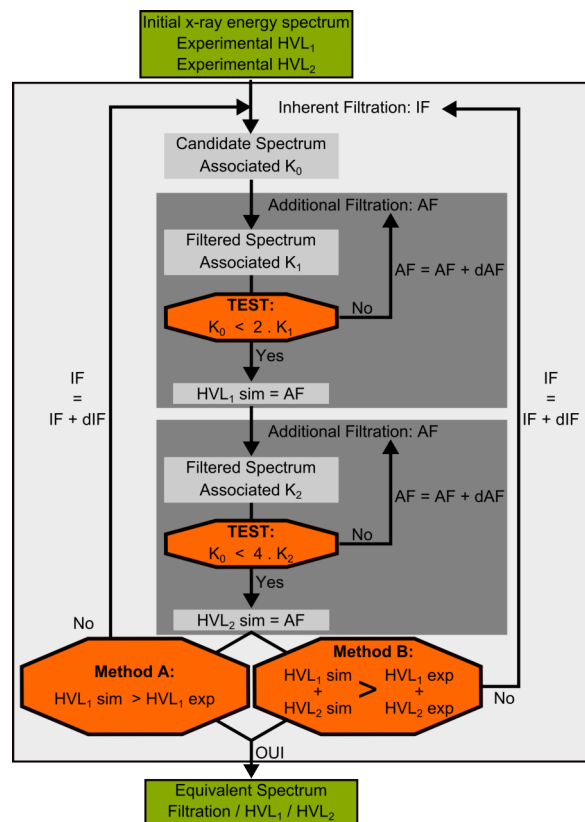

Figure 2: Flowchart for the experimental determination of the CT model.

Both Spekcalc and PENELOPE equivalent spectra have been used in the PENRADIO software to determine the

simulated air KERMA ($K_{air,sim}$) at the CT isocenter. In a static mode, simulated values and the experimental KERMA measured with a NE-2571 ionization chamber have been compared to determine the best suited method to model the X-ray tube.

3.2. Experimental determination of two bowtie filters

The determination of an equivalent bowtie filter consists in obtaining the aluminium thickness as a function of θ which attenuates the equivalent spectrum in the same manner that the actual bowtie filter. The equivalent bowtie filter has also been determined using a program based on Turner[24] work. Two inputs are necessary to run the program:

a) the equivalent spectrum previously generated;

b) experimental profile measurements.

The following steps are repeated for each angle:

1. the ratio (R) of the measured point at θ_i to the measured central points is computed.

2. KERMA (K_0) associated to the equivalent spectrum is calculated.

3. The equivalent spectrum is repetitively filtered by increasing the aluminium sheet thickness (e_{Al}) and its associated KERMA (K_1) is calculated until $K_0 = R.K_1$.

4. The aluminium thickness for θ_i is set to e_{Al};

Both head and body bowtie filter shapes have been determined and designed with PENGEOM, the PENELOPE package that handles the geometry.

3.3. Implementation of the rotation in PENRADIO

To model the effect of x-ray tube motion during an axial or helical scan, the position and direction of each particle stored in the input PSF were transformed before the particle was released for transport in the patient or phantom. Rotational and translational transformations were performed according to the following equations:[16]

$$\beta = \alpha \cdot RAND \qquad (5)$$

$$d = \beta/2\pi \cdot s + z_0 \qquad (6)$$

with α the total gantry angle rotation during the scan, $RAND$ a random value between 0 and 1, s the table increment per gantry rotation and z_0 the start location of the scan. For single axial scans, α and s equal 2π and 0, respectively.

III. Results

Results of dose calculations with the PENRADIO software in CR, IR and CT as well as their validation are presented.

1. Dose calculation in CR and IR

1.1. Validation of the MC models

The results obtained for the validation of the CR and IR tubes are reported in Table 3. The difference between the measurements and the simulations varies between 0.2 and 5.5%.

		CR		IR	
				graphy	scopy
Potential		77 kV	102 kV	74 kV	85 kV
Exp. data (mm Al)		3.70	4.85	4.68	9.37
Sim. data (mm Al)		3.65	5.00	4.95	9.35
Deviation (%)		1.35	3.10	5.50	0.20

Table 3: Measured and simulated HVL used to validate the CR and IR tubes.

1.2. Simulation of organ doses

Measured and simulated doses in the case of a hip conventional radiography and in the case of a fluorography during a cardiac interventional radiology procedure are presented in Table 4, Figure 3 and Figure 4. Errors about 20% are tolerated for medical imaging examinations.

Localization	Measured Dose (mGy)	Simulated Dose (mGy)	Error (%)
Hip	0.233	0.29 ± 0.03	23.6
Lung	0.584	0.56 ± 0.05	3.5

Table 4: Measured and simulated dose for a hip conventional radiography and a fluorography in a cardiac interventional radiography.
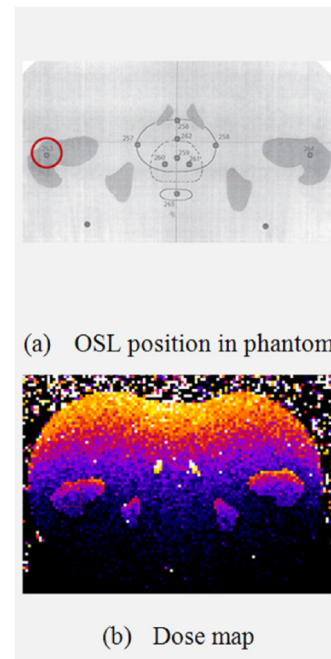

(a) OSL position in phantom

(b) Dose map

Figure 3: Male patient in a hip conventional radiography examination at 77 kV.
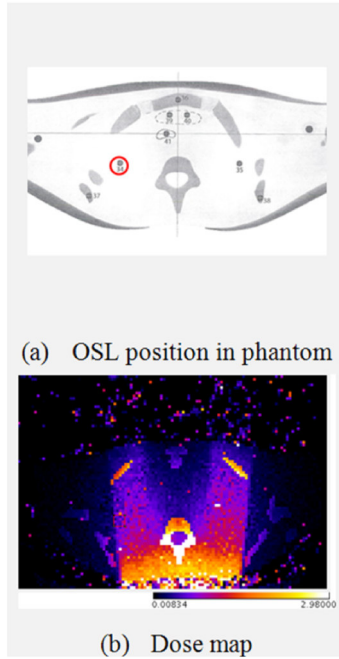
(a) OSL position in phantom

(b) Dose map

Figure 4: Female patient in cardiac interventional radiography examination at 68 kV.

2. Tool adaptation for CT exams

2.1. Equivalent Spectra

Both Spekcalc and MC initial and equivalent spectra are shown in Figure 5. Values of inherent filtration, first and second HVL are reported in Table 5. Values highly depend on the test performed but not on the spectrum type:
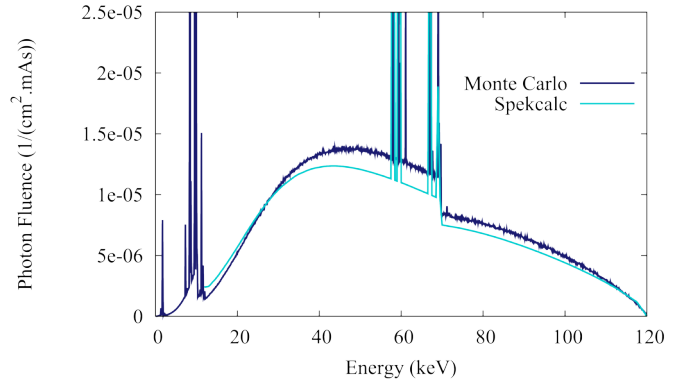
- When only the first HVL is used to determine the inherent filtration, the algorithm converges on the experimental value for the first HVL and a deviation of 7.7% is obtained for the second HVL estimation which are identical for both Spekcalc and MC spectra.

- When both HVL are used together for inherent filtration determination, a deviation of 6.6% and 5.0% can be noticed for the first and the second HVL, respectively. Both HVL values are comparable to each other for both Spekcalc and MC used spectra.

Due to the common use of maximal potential and first HVL to qualify a x-ray tube and a greater global error for the method including both HVL, in the following we chose to use equivalent spectra obtained with the algorithm based on a comparison only of the first HVLs.
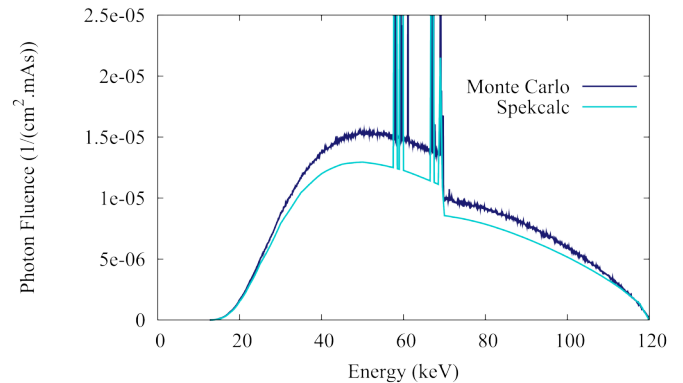
	Exp.	Spekcalc		Monte Carlo	
Method		A	B	A	B
Filtration (mm Al)		2.10	1.67	1.94	1.51
First HVL (mm Al)	6.08	6.08	5.68	6.08	5.69
Second HVL (mm Al)	8.23	8.86	8.64	8.87	8.63

Table 5: Results obtained for the inherent filtration.

Measured air KERMA has been compared to simulated values based on both Spekcalc and MC equivalent spectra

(a) Initial Spectra

(b) Equivalent Spectra

Figure 5: Initial and filtered spectra obtained with the iterative process.

obtained using Method A (Table 6). Simulated values are given in eV/g/photon and are converted into Gray using Equation 3. y_{TX} was set to $3.147 \ 10^{-5}$ for the equivalent filtration of 1.94 mm in aluminium (MC spectrum) and set to $3.144 \ 10^{-5}$ for the equivalent filtration of 2.10 mm in aluminium (Spekcalc spectrum).

$$D_{abs,Gy} = y_{TX} \cdot 1.6 \cdot 10^{-19} \cdot 1000 \cdot N_{elec} \cdot D_{MC,eV/g/shw} \quad (4)$$

Despite the good agreement on the inherent filtration and the two HVL, we note discrepancies of about 25% between the two simulated values (Table 6). The results obtained with the Spekcalc spectrum are closer to the measurements. Further investigations have to be performed to understand these discrepancies. One explanation could be the low interaction probability in air.

Measurements (mGy)	574 ± 15
Monte Carlo (mGy)	714 ± 29
Spekcalc (mGy)	571 ± 25

Table 6: Results obtained for the air KERMA.

2.2. Equivalent Bowtie Filter

Body bowtie filters were designed to cover a large field of view (FOV) corresponding to adult abdominal CT. Head bowtie filters were designed to cover a small FOV corresponding to

head CT or pediatric abdominal CT. According to the fact that in Figure 6, the head bowtie filter (6(a)) appears narrower than the body bowtie filter (6(b)) which corroborates theoretical expectation.
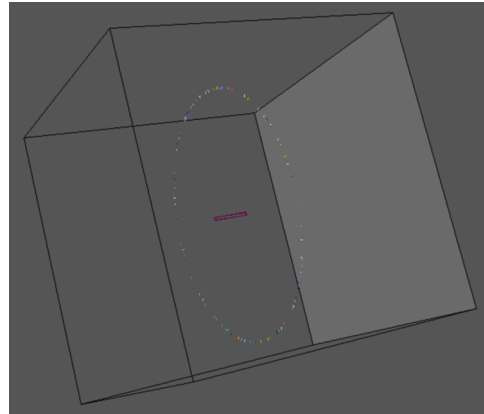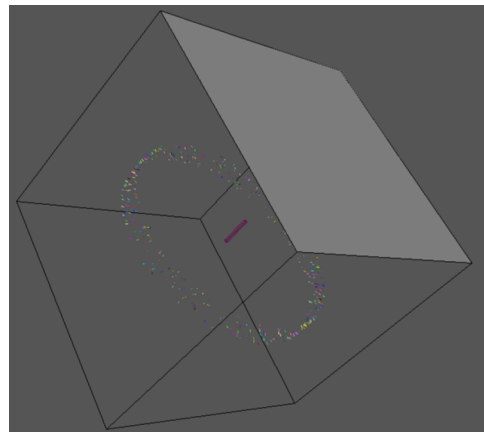

(a) Head bowtie filter

(b) Body bowtie filter

Figure 6: PENGEOM 3D bowtie filter visualisation.

2.3. Geometric validation of the rotation

In Figure 7, multicolour points into the box represent photon emission point. Purple rectangle matches the ionization chamber used for measurements. As we can observe in Figure 7(a) points constitute a circle around the ionization chamber corresponding to an axial CT scan. Figure 7(b) shows a spiral rotation around the ionization chamber. Geometric validations for axial and spiral rotation look promising for further investigations in CT simulations.

IV. Conclusions

The first results obtained with the PENRADIO software are encouraging. The validation of the program is part of the ongoing work for several phantoms and examination procedures in conventional and interventional radiography as well as in CT exams. We expect the same accuracy in the results that we have obtained up to now.

Appendix: Calibration and correction of OSL readings

1. OSL calibration

There are two calibration curves according to the luminescent signal used at the time of reading: beam 1 for high doses and beam 2 for low doses. Readings corrected from the sensitivity of each OSL are used. Once this calibration is made the uncorrected air dose is obtained.

2. Energy response

We determine the average energy of photons arriving on the OSL with a Monte Carlo simulation. The correction factor

(a) Axial rotation

(b) Spiral rotation

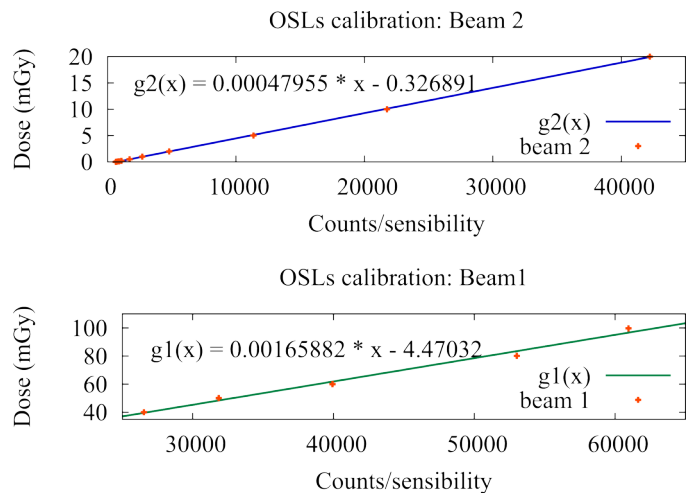**Figure 7: Geometric validation of CT rotation.**

Figure 8: OSL calibrations.

is determined using the curve (Figure 9) obtained in a preliminary study performed with a cobalt beam. We then obtain the corrected air dose.

Acknowledgments

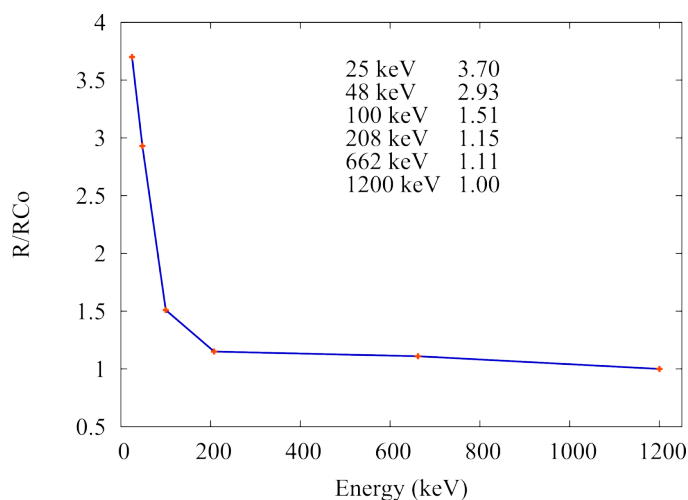|	
25 keV	3.70
48 keV	2.93
100 keV	1.51
208 keV	1.15
662 keV	1.11
1200 keV	1.00

Figure 9: Energy dependance of OSL detectors.

References

1) P. C. Shrimpton, M. C. Hillier, M. A. Lewis, and M. Dunn, "Doses from computed tomography (CT) examinations in the UK - 2003 review," *National Radiological Protection Board* (2005).

2) R. Fazel et al., "Exposure to low-dose ionizing raditaion from medical imaging procedures," *The New England Journal of Medicine*, **361**, *9*, 849-857 (2009).

3) C. Etard, S. Sinno-Tellier, and B. Aubert, "Exposition de la population franÃğaise aux rayonnements ionisants liÃľe aux actes de diagnostic mÃľdical en 2007," (2010).

4) J. Giles, "Study warns of 'avoidable' risks of CT scans," *Nature*, **431**, *7007*, 391 (2004).

5) D. J. Brenner and E. J. Hall, "Computed tomography - an increasing source of radiation exposure," *The New England Journal of Medicine*, **357**, *22*, 2277-2284 (2007).

6) A. B. de Gonzalez et al., "Projected cancer risks from computed tomographic scans performed in the United States in 2007," *Arch Intern Med*, **169**, *22*, 2071-2077 (2009).

7) A. A. of Physicists in Medicine (AAPM), "The measurement, reporting, and management of radiation dose in CT, AAPM report 96," (2008).

8) http://www.stuk.fi.

9) R. Kramer, "CALDose_X - a software tool for the assessmentn of organ and tissue absorbed doses, effective dose and cancer risks in diagnostic radiology," *Phys Med Biol*, **53**, 6437-6459 (2008).

10) "Eff-dose software, X-ray Radiology Dosimetry Program Using NRPB-SR262 National Board Of Health, Denmark, National Institute of Radiation Hygiene," (1995).

11) E. K. Osei and R. Barnett, "Software for the estimation of organ equivalent and effective doses from diagnostic radiology procedures," *J. Radiol. Prot*, **29**, 361-376 (2009).

12) B. Schmitt and W. Kalender, "A fast voxel-based Monte Carlo method for scanner- and patient-specific dose calculations in computed tomography," *Med. Phys*, **36**, 2898-2914 (2009).

13) J. Jarry, J. J. DeMarco, C. H. Cagnon, and M. F. McNitt-Gray, "A Monte Carlo based method to estimate radiation dose from spiral CT: from phantom testing to patient-specific models," *Phys. Med. Bio.*, **48**, 2645-2663 (2009).

14) J. J. DeMarco et al., "A Monte Carlo based method to estimate radiation dose from Multidetector CT : Cylindrical and Anthropomorphic Phantoms," *Phys. Med. Bio.*, **50**, 3989-4004 (2005).

15) P. Deak, M. V. Straten, P. C. Shrimpton, M. Zankl, and W. A. Kalender, "Validation of a Monte Carlo tool for patient-specific dose simulations in multi-slice computed tomography," *European Society of Radiology*, **18**, 759-772 (2008).

16) X. Li et al., "Patient-specific radiation dose and cancer risk estimation in CT: Part I. Development and validation of a Monte Carlo program," *Medical Physics*, **38**, 397-407 (2011).

17) F. Salvat, J. F. Varea, and J. Sempau, *PENELOPE 2006, A Code System for Monte Carlo Simulation of Electron and Photon Transport*, OECD, (Barcelona, Spain) (2006).

18) C. L. Loirec, J. C. G. Hernandez, G. Bonniaud, B. Poumarede, and D. Lazaro, "Dosimetric verification of PENSSART, a new Monte Carlo dose calculation system based on PENELOPE and dedicated to patient-specific treatment quality control," *MCTP2012 - May 15-18 2012 - Sevilla - Spain* (2012).

19) J. DeMarco et al., "A Monte Carlo based method to estimate radiation dose from multidetector CT (MDCT): cylindrical and anthropomorphic phantoms," *Physics in Medicine and Biology*, **50**, 3989-4004 (2005).

20) G. Bueno and O. Deniz, "Fast Monte Carlo simulation on a voxelized human phantom deformed to a patient," *Medical Physics*, **36**, 5162-5174 (2009).

21) P. Jursinic, "Characterization of optically stimulated luminescent dosimeters, OSLDs, for clinical dosimetric measurements," *Medical Physics*, **34**, 4594-4604 (2007).

22) ICRP, "The 1990 Recommendations of the international commission on radiological protection," 1990.

23) ICRP, "The 2007 Recommendations of the international commission on radiological protection," 2007.

24) C. Turner, D. Zhan, H. Kim, and et al., "A method to generate equivalent energy spectra and filtration models based on measurement for multidetector CT Monte Carlo dosimetry simulations," *Medical Physics*, **36**, 2154-2164 (2009).

25) G. Poludniowski, "Calculation of x-ray spectra emerging from an x-ray tube. Part II. X-ray production and filtration in x-ray targets.," *Medical Physics*, **34**, 2175-2186 (2007).